

Non-linear analysis of delamination fracture in functionally graded beams

Victor I. Rizov*

*Department of Technical Mechanics, University of Architecture, Civil Engineering and Geodesy,
1 Chr. Smirnensky blvd., 1046-Sofia, Bulgaria*

(Received August 28, 2016, Revised November 10, 2016, Accepted November 11, 2016)

Abstract. The present paper reports an analytical study of delamination fracture in the Mixed Mode Flexure (MMF) functionally graded beam with considering the material non-linearity. The mechanical behavior of MMF beam is modeled by using a non-linear stress-strain relation. It is assumed that the material is functionally graded along the beam height. Fracture behavior is analyzed by the J-integral approach. Non-linear analytical solution is derived of the J-integral for a delamination located arbitrary along the beam height. The J-integral solution derived is verified by analyzing the strain energy release rate with considering the non-linear material behavior. The effects of material gradient, crack location along the beam height and material non-linearity on the fracture are evaluated. It is found that the J-integral value decreases with increasing the upper crack arm thickness. Concerning the influence of material gradient on the non-linear fracture, the analysis reveals that the J-integral value decreases with increasing the ratio of modulus of elasticity in the lower and upper edge of the beam. It is found also that non-linear material behavior leads to increase of the J-integral value. The present study contributes for the understanding of fracture in functionally graded beams that exhibit material non-linearity

Keywords: functionally graded materials; fracture; non-linear material behavior; beam theory

1. Introduction

Due to smooth spatial variation of material properties, functionally graded materials have a number of advantages over the homogeneous structural materials. For instance, one can achieve optimum performance of a component to external influence (mechanical loading, temperature difference, etc.) by tailoring the variation of material properties. Therefore, recently, the use of functionally graded materials has increased in many engineering applications (Koizumi 1993, Markworth *et al.* 1995, Suresh and Mortensen 1998, Hirai and Chen 1999, Lu *et al.* 2009, Gasik 2010, Nemat-Allal *et al.* 2011, Ivanov and Stoyanov 2012, Ivanov and Draganov 2014, Ivanov *et al.* 2016, Bohidar *et al.* 2014).

Fracture is one of the most common failure modes in functionally graded materials. The existence of cracks can drastically reduce the strength, stiffness and stability of a structure

*Corresponding author, Professor, E-mail: v_rizov_fhe@uacg.bg

composed by functionally graded material. Therefore, better understanding of the fracture behaviour is of great importance for the structural design and development of new functionally graded material systems. This fact is reflected by the significant number of papers published in the field of fracture mechanics of these novel materials (Pei and Asaro 1997, Tilbrook *et al.* 2005, Carpinteri and Pugno 2006, Upadhyay and Simha 2007, Zhang *et al.* 2013).

Analytical investigations have been carried-out of semi-infinite cracks in a strip of functionally graded material by using the methods of linear-elastic fracture mechanics (Pei and Asaro 1997). The loading has been applied on the edge of the strip. Solutions for stress intensity factors have been obtained. The solutions derived have been extended for a strip of an orthotropic functionally graded material. Possibilities have been considered for development of a fracture criterion for functionally graded materials.

Studies have been reviewed of the linear-elastic fracture behavior of functionally graded composite materials by Tilbrook, Moon and Hoffman (2005). Analyses have been presented of the stress intensity factors. Cracks oriented both parallel and perpendicular to the gradient direction have been investigated. Works in the field of fatigue fracture behavior have also been summarized.

Linear-elastic fracture analyses have been performed of structures composed by functionally graded materials by Carpinteri and Pugno (2006). Functionally graded plates in tension and beams under three-point bending have been considered. Stress intensity factors have been investigated. An engineering method has been developed for evaluation of the strength of structures corresponding to the unstable brittle crack propagation.

Fracture behavior has been studied of functionally graded linear-elastic beams loaded in three-point bending (Upadhyay and Simha 2007). Equivalent homogeneous beams of variable depth have been suggested for evaluation of the stress intensity factor. The compliance method has been applied in the analysis. It has been shown that equivalent beams are quite efficient for engineering design analyses of cracked functionally graded linear-elastic structures.

It can be summarized that fracture behavior of functionally graded beam structures has been analyzed mainly assuming linear-elastic stress-strain relation. However, in reality, the stress-strain relation can be non-linear. Therefore, the objective of present work is to perform a theoretical study of delamination fracture in the functionally graded MMF beam configuration assuming non-linear material behavior. The J -integral approach is applied in the non-linear fracture analysis. The influence of material gradient and crack location along the beam height on the non-linear fracture is investigated.

It should be noted that, in principle, fracture in beams can be analyzed by analytical methods or by finite element models. The analytical solutions are very useful for parametric investigations. Besides, the analytical solutions have lower computational cost in comparison with finite element models. Therefore, fracture behavior is analyzed analytically in the present paper.

2. Non-linear fracture study

The present article is concerned with theoretical study of non-linear fracture in the functionally graded MMF beam configuration shown schematically in Fig. 1. The beam is loaded by a transverse force, F , applied in the mid-span. There is a delamination crack of length a located arbitrary along the beam height (it should be noted that the present study is motivated also by the fact that functionally graded materials can be built up layer by layer (Bohidar *et al.* 2014), which is a premise for appearance of delamination cracks between layers). The upper and

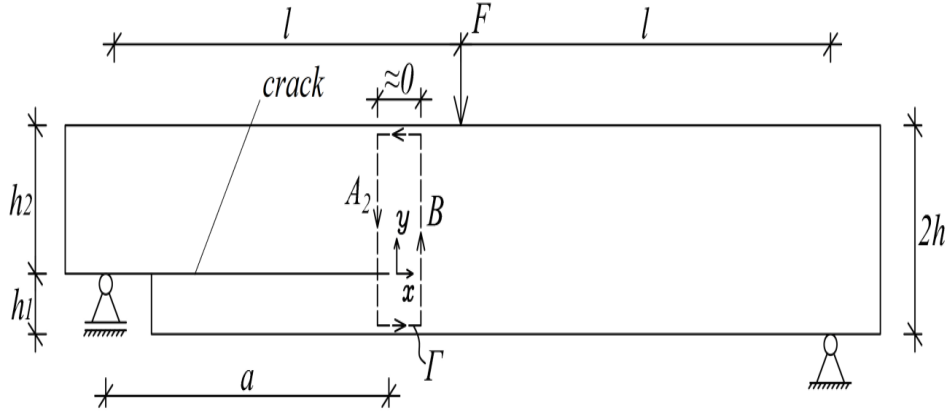


Fig. 1 The MMF beam configuration

lower crack arm thicknesses are h_1 and h_2 , respectively (Fig. 1). The lower crack arm is stress free. The beam has a rectangular cross-section of width, b , and height, $2h$.

In the fracture analysis performed, the mechanical response of beam is described by the following non-linear stress-strain relation (Petrov 2014)

$$\sigma = E\varepsilon - R_1\varepsilon^{s_1} - R_2\varepsilon^{s_2} \quad (1)$$

where σ is the stress, ε is the strain, E is the modulus of elasticity, R_1 , R_2 , s_1 and s_2 are material properties. The stress-strain curve is symmetric with respect to tension and compression (Fig. 2). The present analysis is based on the small strain assumption (it should be noted that this assumption has been frequently used in fracture analyses of functionally graded materials (Pei and Asaro 1997, Carpinteri and Pugno 2006, Upadhyay and Simha 2007)). It is also assumed that the value of E varies linearly along the beam height from E_0 in the upper edge to E_1 in the lower edge of beam cross-section, i.e., the material is functionally graded along the beam height. Thus, E was written as

$$E = E_0 + \frac{E_1 - E_0}{2h}(h + z_3) \quad (2)$$

where the z_3 -axis originates from the beam cross-section centre and is directed downwards.

The non-linear fracture behavior of functionally graded MMF beam configuration is analyzed with the help of J -integral approach (Anlas *et al.* 2000)

$$J = \int_{\Gamma} \left[u_0 \cos \alpha - \left(p_x \frac{\partial u}{\partial x} + p_y \frac{\partial v}{\partial x} \right) \right] ds - \int_A \frac{\partial u_0}{\partial x} q dA \quad (3)$$

where Γ is a contour of integration going from the lower crack face to the upper crack face in the counter clockwise direction, u_0 is the strain energy density, α is the angle between the outwards normal vector to the contour of integration and the crack direction, p_x and p_y are the components of stress vector, u and v are the components of displacement vector with respect to the crack tip coordinate system xy (x is directed along the crack), ds is a differential element along the contour, A is the area enclosed by that contour, q is a weight function with a value of unity at the crack tip,

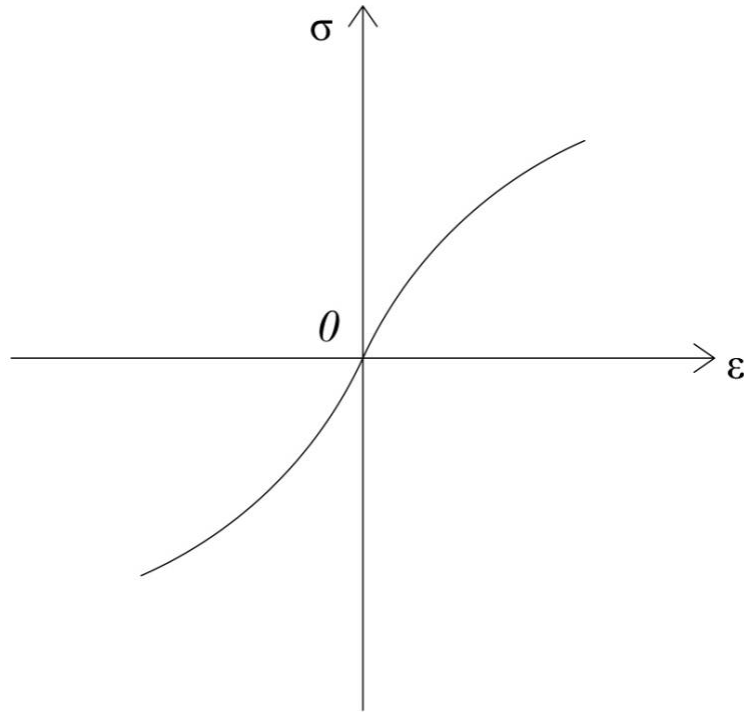


Fig. 2 Non-linear stress-strain curve

zero along the contour and arbitrary elsewhere. It should be specified that the partial derivative $\partial u_0/\partial x$ exists only if the material property is an explicit function of x (Anlas *et al.* 2000).

It should be noted that the fracture analysis performed holds for non-linear elastic material behavior. However, the analysis is applicable also for elastic-plastic behavior, if the external load magnitude increases only, i.e., if the beam considered undergoes active deformation (Lubliner 2006, Chakrabarty 2006).

The J -integral is solved by using an integration contour that coincides with the beam cross-sections behind and ahead of the crack tip as illustrated in Fig. 1. The lower crack arm is stress free. Thus, the J -integral value in the lower crack arm is zero. It is obvious that the J -integral has non-zero values in segments A_2 and B of the integration contour (Fig. 1). Therefore, the J -integral value can be obtained by summation, i.e.,

$$J = J_{A_2} + J_B \quad (4)$$

where J_{A_2} and J_B are the J -integral values in segments A_2 and B , respectively.

The integration contour segment, A_2 , coincides with the upper crack arm cross-section behind the crack tip (Fig. 1). The cross-sectional bending moment in segment, A_2 , is obtained as

$$M = \frac{F}{2}a \quad (5)$$

The stress distribution in the upper crack arm cross-section is shown schematically in Fig. 3. The J -integral components in segment, A_2 , are written as

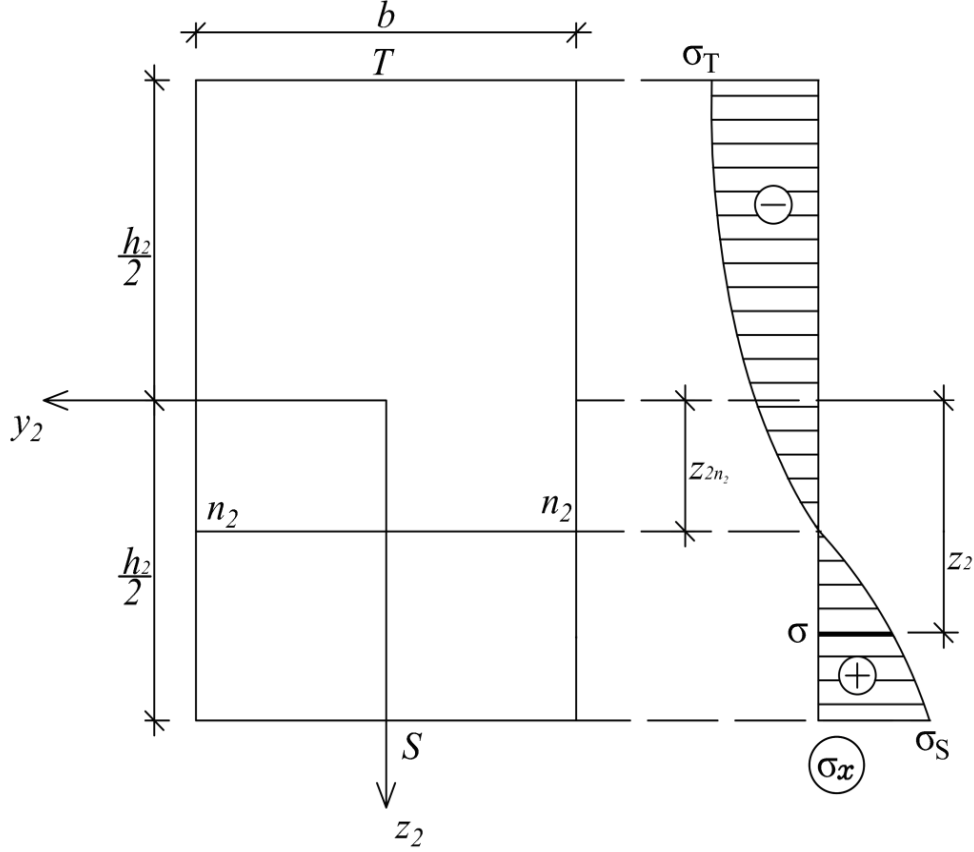


Fig. 3 Diagram of stresses in the upper crack arm cross-section

$$p_x = -\sigma = -E\varepsilon + R_1\varepsilon^{s_1} + R_2\varepsilon^{s_2}, \quad p_y = 0, \quad (6)$$

$$ds = dz_2, \quad \cos \alpha = -1, \quad (7)$$

where the z_2 -coordinate varies in the interval $[-h_2/2, h_2/2]$. The axis, z_2 , is shown in Fig. 3.

The strain energy density, u_0 , is equal to the area enclosed by the stress-strain curve (refer to Fig. 4)

$$u_0 = \int_0^\varepsilon \sigma d\varepsilon \quad (8)$$

After substitution of Eq. (1) in Eq. (8), the strain energy density is obtained as

$$u_0 = \frac{E\varepsilon^2}{2} - \frac{R_1\varepsilon^{s_1+1}}{s_1+1} - \frac{R_2\varepsilon^{s_2+1}}{s_2+1} \quad (9)$$

It is assumed that the Bernoulli's hypothesis for plane sections is applicable in the present

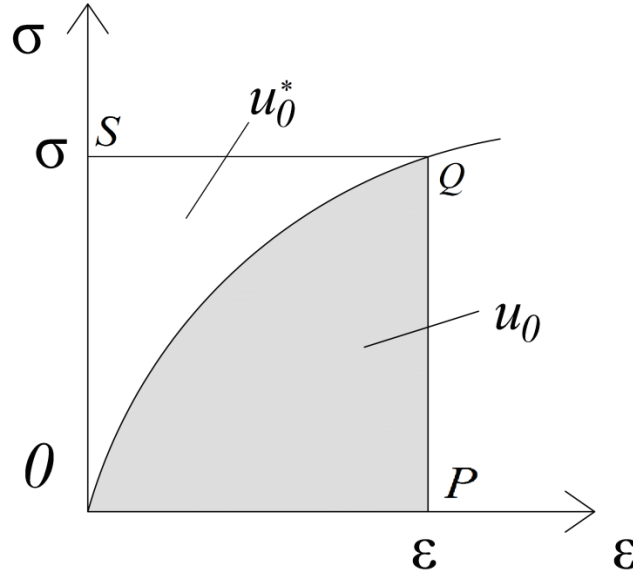


Fig. 4 Strain energy density, u_0 , and complimentary strain energy density, u_0^*

analysis, since the span to height ratio of beam considered is large. Therefore, the strains are distributed linearly along the beam height, i.e.,

$$\varepsilon = \kappa_2 (z_2 - z_{2n_2}) \quad (10)$$

where κ_2 and z_{2n_2} are the curvature and neutral axis coordinate of upper crack ram cross-section behind the crack tip, respectively (the neutral axis shifts from the centroid, because the material is functionally graded transversally to the beam). It should be mentioned that the Bernoulli's hypothesis for plane sections has been widely applied when analyzing fracture in functionally graded beams (Pei and Asaro 1997, Carpinteri and Pugno 2006, Upadhyay and Simha 2007).

The following equations for equilibrium of cross-section, A_2 , are used to determine κ_2 and z_{2n_2}

$$N = \int_{-\frac{h_2}{2}}^{\frac{h_2}{2}} \sigma(\varepsilon) b dz_2 = 0 \quad (11)$$

$$M = \int_{-\frac{h_2}{2}}^{\frac{h_2}{2}} \sigma(\varepsilon) b z_2 dz_2 \quad (12)$$

where N and M are the axial force and the bending moment in the upper crack arm behind the crack tip, respectively (obviously, $N=0$ (Fig. 1)). The variation of E along the upper crack arm

cross-section height is written as (refer to Eq. (2))

$$E = E_0 + \frac{E_1^L - E_0}{h_2} \left(\frac{h_2}{2} + z_2 \right) \quad (13)$$

where

$$E_1^L = E_0 + \frac{E_1 - E_0}{2h} h_2 \quad (14)$$

is the value of E in the lower edge of the upper crack arm.

After substitution of Eq. (1), Eq. (10) and Eq. (13) and solving the integrals, the equilibrium equations are written as

$$\begin{aligned} & \frac{\kappa_2}{2} \left[\frac{1}{2} (E_0 + E_1^L) + \frac{1}{h_2} (E_1^L - E_0) z_{2n_2} \right] \left[\left(\frac{h_2}{2} - z_{2n_2} \right)^2 - \left(-\frac{h_2}{2} - z_{2n_2} \right)^2 \right] + \\ & + \frac{\kappa_2}{3h_2} (E_1^L - E_0) \left[\left(\frac{h_2}{2} - z_{2n_2} \right)^3 - \left(-\frac{h_2}{2} - z_{2n_2} \right)^3 \right] - \\ & - \frac{\kappa_2^{s_1}}{s_1 + 1} R_1 \left[\left(\frac{h_2}{2} - z_{2n_2} \right)^{s_1+1} - \left(-\frac{h_2}{2} - z_{2n_2} \right)^{s_1+1} \right] - \\ & - \frac{\kappa_2^{s_2}}{s_2 + 1} R_2 \left[\left(\frac{h_2}{2} - z_{2n_2} \right)^{s_2+1} - \left(-\frac{h_2}{2} - z_{2n_2} \right)^{s_2+1} \right] = 0 \end{aligned} \quad (15)$$

$$\begin{aligned} M = \kappa_2 b \left\{ E_0 \left[\frac{1}{3} \left[\left(\frac{h_2}{2} - z_{2n_2} \right)^3 - \left(-\frac{h_2}{2} - z_{2n_2} \right)^3 \right] + \right. \right. \\ \left. \left. + \frac{1}{2} \left[\left(\frac{h_2}{2} - z_{2n_2} \right)^2 z_{2n_2} - \left(-\frac{h_2}{2} - z_{2n_2} \right)^2 z_{2n_2} \right] \right\} + \right. \\ \left. + \frac{1}{2} (E_1^L - E_0) \left[\frac{1}{3} \left[\left(\frac{h_2}{2} - z_{2n_2} \right)^3 - \left(-\frac{h_2}{2} - z_{2n_2} \right)^3 \right] + \right. \right. \\ \left. \left. + \frac{z_{2n_2}}{2} \left[\left(\frac{h_2}{2} - z_{2n_2} \right)^2 - \left(-\frac{h_2}{2} - z_{2n_2} \right)^2 \right] \right] \right\} + \end{aligned}$$

$$\begin{aligned}
& + \frac{1}{h_2} (E_1^L - E_0) \left\{ \frac{1}{4} \left[\left(\frac{h_2}{2} - z_{2n_2} \right)^4 - \left(-\frac{h_2}{2} - z_{2n_2} \right)^4 \right] + \right. \\
& \quad \left. + \frac{2z_{2n_2}}{3} \left[\left(\frac{h_2}{2} - z_{2n_2} \right)^3 - \left(-\frac{h_2}{2} - z_{2n_2} \right)^3 \right] + \right. \\
& \quad \left. + \frac{z_{2n_2}^2}{2} \left[\left(\frac{h_2}{2} - z_{2n_2} \right)^2 - \left(-\frac{h_2}{2} - z_{2n_2} \right)^2 \right] \right\} - \\
& - \kappa_2^{s_1} b R_1 \left\{ \frac{1}{s_1 + 2} \left[\left(\frac{h_2}{2} - z_{2n_2} \right)^{s_1+2} - \left(-\frac{h_2}{2} - z_{2n_2} \right)^{s_1+2} \right] + \right. \\
& \quad \left. + \frac{1}{s_1 + 1} \left[\left(\frac{h_2}{2} - z_{2n_2} \right)^{s_1+1} z_{2n_2} - \left(-\frac{h_2}{2} - z_{2n_2} \right)^{s_1+1} z_{2n_2} \right] \right\} - \\
& - \kappa_2^{s_2} b R_2 \left\{ \frac{1}{s_2 + 2} \left[\left(\frac{h_2}{2} - z_{2n_2} \right)^{s_2+2} - \left(-\frac{h_2}{2} - z_{2n_2} \right)^{s_2+2} \right] + \right. \\
& \quad \left. + \frac{1}{s_2 + 1} \left[\left(\frac{h_2}{2} - z_{2n_2} \right)^{s_2+1} z_{2n_2} - \left(-\frac{h_2}{2} - z_{2n_2} \right)^{s_2+1} z_{2n_2} \right] \right\} \quad (16)
\end{aligned}$$

Obviously, at $R_1=R_2=0$, the non-linear stress-strain relation Eq. (1) transforms into the Hooke's law. This means that at $R_1=R_2=0$ Eq. (16) should transform in the formula for curvature of linear-elastic beam. Indeed, by substitution of $R_1=R_2=0$ and $E_0 = E_1^L = E$ in Eq. (16), we obtain

$$\kappa_2 = \frac{12M}{Eb h_2^3} \quad (17)$$

Eq. (17) coincides with the known expression for curvature of homogeneous linear-elastic beam.

The MatLab computer program should be used to solve Eqs. (15) and (16) as an algebraic system with unknowns to κ_2 and z_{2n_2} .

The partial derivative in the first integral in Eq. (3) is expressed as

$$\frac{\partial u}{\partial x} = \varepsilon = \kappa_2 (z_2 - z_{2n_2}) \quad (18)$$

where κ_2 and z_{2n_2} are determined from Eq. (15) and Eq. (16).

The partial derivative in the second integral in Eq. (3) is written as

$$\frac{\partial u_0}{\partial x} = 0 \quad (19)$$

since the strain energy density is not an explicit function of x (the material property E does not depend on x , because the material is functionally graded transversally to the beam only (refer to Eq. (2)).

After substitution of Eqs. (6), (7), (9), (10), (13), (18) and (19) in Eq. (3), the J -integral solution in segment, A_2 , of the integration contour is written as

$$\begin{aligned} J_{A_2} = & \frac{\kappa_2^2 E_0}{6} \left[\left(-\frac{h_2}{2} - z_{2n_2} \right)^3 - \left(\frac{h_2}{2} - z_{2n_2} \right)^3 \right] + \\ & + \frac{\kappa_2^2 (E_1^L - E_0)}{2} \left\{ \frac{1}{6} \left[\left(-\frac{h_2}{2} - z_{2n_2} \right)^3 - \left(\frac{h_2}{2} - z_{2n_2} \right)^3 \right] + \right. \\ & \quad \left. + \frac{1}{4h_2} \left[\left(-\frac{h_2}{2} - z_{2n_2} \right)^4 - \left(\frac{h_2}{2} - z_{2n_2} \right)^4 \right] + \right. \\ & \quad \left. + \frac{z_{2n_2}}{3h_2} \left[\left(-\frac{h_2}{2} - z_{2n_2} \right)^3 - \left(\frac{h_2}{2} - z_{2n_2} \right)^3 \right] \right\} + \\ & + \kappa_2^2 \left\{ \frac{E_0}{3} \left[\left(\frac{h_2}{2} - z_{2n_2} \right)^3 - \left(-\frac{h_2}{2} - z_{2n_2} \right)^3 \right] + \right. \\ & \quad \left. + \frac{E_1^L - E_0}{6} \left[\left(\frac{h_2}{2} - z_{2n_2} \right)^3 - \left(-\frac{h_2}{2} - z_{2n_2} \right)^3 \right] + \right. \\ & \quad \left. + \frac{E_1^L - E_0}{4h_2} \left[\left(\frac{h_2}{2} - z_{2n_2} \right)^4 - \left(-\frac{h_2}{2} - z_{2n_2} \right)^4 \right] + \right. \\ & \quad \left. + \frac{z_{2n_2} (E_1^L - E_0)}{3h_2} \left[\left(\frac{h_2}{2} - z_{2n_2} \right)^3 - \left(-\frac{h_2}{2} - z_{2n_2} \right)^3 \right] \right\} - \end{aligned} \quad (20)$$

$$-\frac{R_1 s_1 \kappa_2^{s_1+1}}{(s_1+1)(s_1+2)} \left[\left(\frac{h_2}{2} - z_{2n_2} \right)^{s_1+2} - \left(-\frac{h_2}{2} - z_{2n_2} \right)^{s_1+2} \right] -$$

$$-\frac{R_2 s_2 \kappa_2^{s_2+1}}{(s_2+1)(s_2+2)} \left[\left(\frac{h_2}{2} - z_{2n_2} \right)^{s_2+2} - \left(-\frac{h_2}{2} - z_{2n_2} \right)^{s_2+2} \right]$$

The integration in segment B is performed in a similar way (segment B coincides with the MMF beam cross-section ahead of the crack tip as shown in Fig. 1). The J -integral components are written as

$$p_x = \sigma = E\varepsilon - R_1 \varepsilon^{s_1} - R_2 \varepsilon^{s_2}, \quad p_y = 0, \quad (21)$$

$$ds = -dz_3, \quad \cos \alpha = 1, \quad (22)$$

$$\frac{\partial u}{\partial x} = \varepsilon = \kappa_3 (z_3 - z_{3n_3}), \quad (23)$$

where κ_3 and z_{3n_3} are the curvature and the neutral axis coordinate in the beam cross-section ahead of the crack tip. Eqs. (15) and (16) can be used to determine κ_3 and z_{3n_3} . For this purpose, κ_2 , h_2 , z_{2n_2} and E_1^L have to be replaced with κ_3 , $2h$, z_{3n_3} and E_1 , respectively. Then Eqs. (15) and (16) should be solved with respect to κ_3 and z_{3n_3} by using the MatLab computer program.

Eqs. (2), (9), (13), (19), (21), (22) and (23) are substituted in Eq. (3). The J_B solution is obtained as

$$J_B = -\frac{\kappa_3^2 E_0}{6} \left[(-h - z_{3n_3})^3 - (h - z_{3n_3})^3 \right] -$$

$$-\frac{\kappa_3^2 (E_1 - E_0)}{2} \left\{ \frac{1}{6} \left[(-h - z_{3n_3})^3 - (h - z_{3n_3})^3 \right] + \right.$$

$$+\frac{1}{8h} \left[(-h - z_{3n_3})^4 - (h - z_{3n_3})^4 \right] +$$

$$+\frac{z_{3n_3}}{6h} \left[(-h - z_{3n_3})^3 - (h - z_{3n_3})^3 \right] \left. \right\} -$$

$$-\kappa_3^2 \left\{ \frac{E_0}{3} \left[(h - z_{3n_3})^3 - (-h - z_{3n_3})^3 \right] + \right.$$

$$\begin{aligned}
 & + \frac{E_1 - E_0}{6} \left[(h - z_{3n_3})^3 - (-h - z_{3n_3})^3 \right] + \\
 & + \frac{E_1 - E_0}{8h} \left[(h - z_{3n_3})^4 - (-h - z_{3n_3})^4 \right] + \\
 & + \frac{z_{3n_3}(E_1 - E_0)}{6h} \left[(h - z_{3n_3})^3 - (-h - z_{3n_3})^3 \right] \left. \right\} + \\
 & + \frac{R_1 s_1 \kappa_3^{s_1+1}}{(s_1 + 1)(s_1 + 2)} \left[(h - z_{3n_3})^{s_1+2} - (-h - z_{3n_3})^{s_1+2} \right] + \\
 & + \frac{R_2 s_2 \kappa_3^{s_2+1}}{(s_2 + 1)(s_2 + 2)} \left[(h - z_{3n_3})^{s_2+2} - (-h - z_{3n_3})^{s_2+2} \right]
 \end{aligned}$$

The J -integral final non-linear solution is found by substitution of Eq. (20) and Eq. (24) in Eq. (4). The formula obtained is cumbersome and is not shown here.

It should be mentioned that by substitution of $R_1=R_2=0$, $E_0=E_1=E$ and $h_1=h_2=h$ in the J -integral non-linear solution derived, we obtain

$$J = \frac{21F^2 a^2}{16Eh^3 b^2} \quad (25)$$

Eq. (25) coincides with the formula for strain energy release rate in the homogeneous linear-elastic MMF configuration, when the crack is located in the beam mid-plane (Szekrenyes 2012).

The J -integral non-linear solution derived in the present paper is verified by analyzing the strain energy release rate in the functionally graded MMF beam with considering the non-linear material behavior. For this purpose, a small crack length increase, Δa , is assumed (the external loading is kept constant). The crack area increase, ΔA_a , is written as

$$\Delta A_a = b\Delta a \quad (26)$$

The strain energy release rate associated with ΔA_a is defined as

$$G = \frac{\Delta W_{ext} - \Delta U}{\Delta A_a} \quad (27)$$

where ΔW_{ext} and ΔU are the changes of external work and strain energy, respectively. The change of external work is expressed as

$$\Delta W_{ext} = \Delta U^* + \Delta U \quad (28)$$

where ΔU^* is the change of complimentary strain energy. By combining of Eqs. (27) and (28), we obtain

$$G = \frac{\Delta U^*}{\Delta A_a} \quad (29)$$

where

$$\Delta U^* = U_a^* - U_b^* \quad (30)$$

Here, U_b^* and U_a^* are the complimentary strain energies before and after the increase of crack, respectively. By substitution of Eqs. (26) and (30) in Eq. (29), we find

$$G = \frac{U_a^* - U_b^*}{b\Delta a} \quad (31)$$

The complimentary strain energy before the increase of crack is written as

$$U_b^* = \Delta ab \int_{-h}^h u_0^* dz_3 \quad (32)$$

where the complimentary strain energy density, u_0^* , in Eq. (32) is equal to the area OQS that supplements the area OPQ enclosed by the stress-strain curve to a rectangle (Fig. 4). Thus, the complimentary strain energy density is obtained as

$$u_0^* = \sigma \varepsilon - u_0 \quad (33)$$

where the stress, σ , and the strain energy density, u_0 , are determined by Eqs. (1) and (9), respectively.

The complimentary strain energy after the increase of crack is calculated as

$$U_a^* = \Delta ab \int_{-\frac{h_2}{2}}^{\frac{h_2}{2}} u_0^* dz_2 \quad (34)$$

By substitution of Eqs. (32) and (34) in Eq. (31), we derive

$$G = \int_{-\frac{h_2}{2}}^{\frac{h_2}{2}} u_0^* dz_2 - \int_{-h}^h u_0^* dz_3 . \quad (35)$$

By combining of Eqs. (1), (9), (23), (33) and Eq. (35), we derive the formula for strain energy release rate that is exact match of the J -integral non-linear solution. This fact is a verification of the non-linear fracture analysis performed the present paper.

3. Influence of material gradient, crack location and material non-linearity on the fracture

First, the influence is analyzed of material gradient and crack location along the beam height on the non-linear fracture behavior of functionally graded MMF configuration. For this purpose, calculations are performed by using the J -integral non-linear solution derived in the present paper.

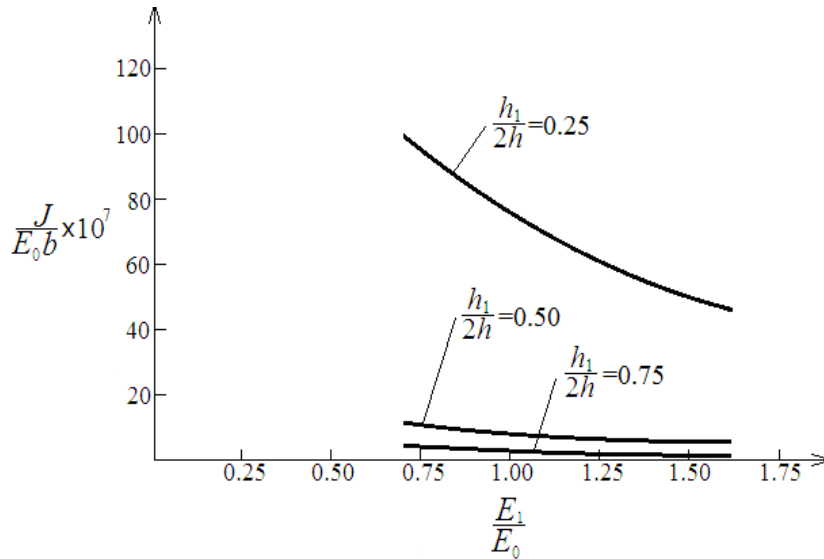


Fig. 5 The J -integral value in non-dimensional form plotted against E_1/E_0 ratio for $h_1/2h=0.25, 0.5$ and 0.75

The calculations are carried-out assuming that $h=0.002$ m, $b=0.02$ m, $a=0.03$ m and $F=300$ N. In these calculations, the material gradient and the crack position along the beam height are characterized by E_1/E_0 and $h_2/2h$ ratios, respectively (refer to Eq. (2) and Fig. 1). It should be specified that E_0 is kept constant in the calculations (thus, E_1 is varied in order to obtain various E_1/E_0 ratios). The J -integral values generated by the calculations are presented in non-dimensional form by using the formula $J_N=J/(E_0b)$. The effects of material gradient and crack location are illustrated in Fig. 5 where the J -integral value is plotted against E_1/E_0 ratio for $h_2/2h=0.25, 0.50$ and 0.75 at $R_1/E_0=0.2$, $R_2/E_0=0.3$, $s_1=0.7$ and $s_2=0.8$. The curves in Fig. 5 indicate that the J -integral value decreases with increasing E_1/E_0 ratio. This finding is explained with increase of the MMF beam stiffness. Also, it can be observed in Fig. 5 that increase of $h_2/2h$ ratio leads to decrease of the J -integral value. This finding is attributed to increase of the upper crack arm stiffness.

It is interesting to investigate the influence of non-linear material behavior on the fracture in the functionally graded MMF beam. For this purpose, the J -integral values calculated by using the non-linear solution derived are plotted in non-dimensional form against the external load, F , for $E_1/E_0=1.5$, $h_2/2h=0.25$, $R_1/E_0=0.2$ and $R_2/E_0=0.3$ as shown in Fig. 6. The J -integral values obtained assuming linear-elastic material behavior of the functionally graded beam are also plotted in Fig. 6 for comparison (the linear-elastic J -integral solution is derived by substitution of $R_1=R_2=0$ in the non-linear solution).

The curves shown in Fig. 6 indicate that the J -integral value increases, when the material non-linearity is taken into account. Therefore, the non-linear material behavior has to be considered in fracture mechanics based safety design of functionally graded structural members.

4. Conclusions

Delamination fracture behavior of the MMF functionally graded beam is studied analytically

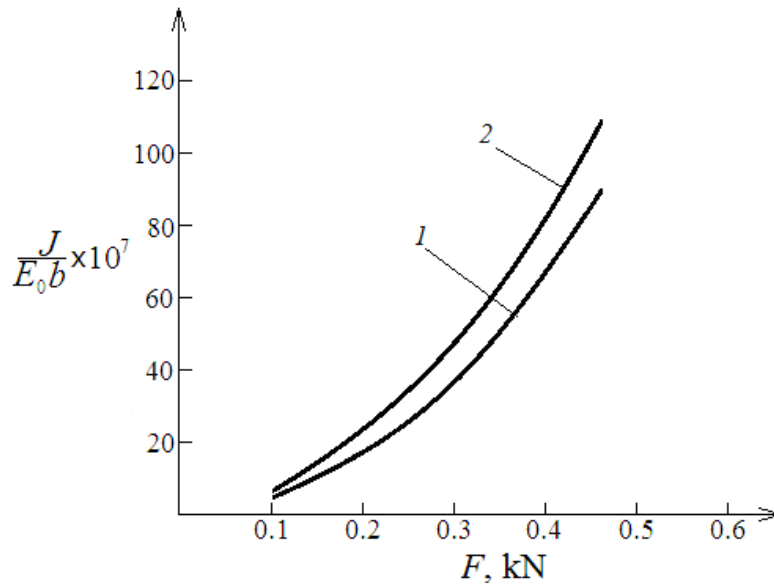


Fig. 6 The J -integral value in non-dimensional form plotted against the external load, F (curve 1-linear-elastic material behavior, curve 2-non-linear material behavior)

with taking into account the material non-linearity. It is assumed that the material is functionally graded transversally to the beam (linear variation of the modulus of elasticity along the beam height is considered). The mechanical behavior of MMF beam is modeled analytically by using a non-linear stress-strain relation. Fracture is analyzed by the J -integral approach. In order to derive the J -integral non-linear solution, the curvature and the neutral axis coordinate of beam are determined. The J -integral is solved analytically for a delamination crack located arbitrary along the beam height. In order to verify the solution obtained, the strain energy release rate is analyzed with considering the material non-linearity. The effects of material gradient, crack location and the material non-linearity on the fracture behavior are evaluated. It is found that the J -integral value decreases with increasing the upper crack arm thickness (the lower crack arm is stress free). This finding is attributed to increase of the upper crack arm bending stiffness. The analysis reveals that the J -integral value decreases with increasing the ratio of modulus of elasticity in the lower and upper edge of the functionally graded beam. Also, it is found that the non-linear material behavior leads to increase of the J -integral value (this finding indicates that the material non-linearity should be taken into account in fracture mechanics based safety design of functionally graded structural members). The results obtained can be applied for optimization of the functionally graded beam structure with respect to the fracture performance. The present study contributes for the understanding of fracture behavior of functionally graded beams exhibiting material non-linearity.

Acknowledgments

The present study was supported financially by the Research and Design Centre (CNIP) of the UACEG, Sofia (Contract BN-189/2016).

References

- Anlas, G., Santare, M.H. and Lambros, J. (2000), "Numerical calculation of stress intensity factors in functionally graded materials", *Int. J. Fract.*, **104**(1), 131-143.
- Bohidar, S.K., Sharma, R. and Mishra, P.R. (2014), "Functionally graded materials: a critical review", *Int. J. Res.*, **1**(7), 289-301.
- Carpinteri, A. and Pugno, N. (2006), "Cracks in re-entrant corners in functionally graded materials", *Eng. Fract. Mech.*, **73**(6), 1279-1291.
- Chakrabarty, J. (2006), *Theory of Plasticity*, Elsevier Butterworth-Heinemann, Oxford.
- Gasik, M.M. (2010), "Functionally graded materials: Bulk processing techniques", *Int. J. Mater. Prod. Technol.*, **39**(1-2), 20-29.
- Hirai, T. and Chen, L. (1999), "Recent and prospective development of functionally graded materials in Japan", *Mater. Sci. Forum*, **308-311**(4), 509-514.
- Ivanov, I. and Draganov, I. (2014), "Influence and simulation of laminated glass subjected to low-velocity impact", *Mech. Mach.*, **110**, 89-94.
- Ivanov, V., Velchev, D.S., Georgiev, N.G., Ivanov, I.D. and Sadowski, T. (2016), "A plate finite element for modelling of triplex laminated glass and comparison with other computational models", *Meccan.*, **51**(2), 341-358.
- Ivanov, Y. and Stoyanov, V. (2012), "High technologies and new construction materials in civil engineering", *Proceedings of the 1st International Conference of the European Polytechnical University*, Pernik, Bulgaria, June.
- Koizumi, M. (1993), "The concept of FGM ceramic trans", *Function. Grad. Mater.*, **34**(1), 3-10.
- Lubliner, J. (2006), *Plasticity Theory*, Revised Edition, University of California, Berkeley, U.S.A.
- Lu, C.F., Lim, C.W. and Chen, W.Q. (2009), "Semi-analytical analysis for multi-dimensional functionally graded plates: 3-D elasticity solutions", *Int. J. Num. Meth. Eng.*, **79**(3), 25-44.
- Markworth, A.J., Ramesh, K.S. and Parks, J.W.P. (1995), "Review: Modeling studies applied to functionally graded materials", *J. Mater. Sci.*, **30**(3), 2183-2193.
- Nemat-Allal, M.M., Ata, M.H., Bayoumi, M.R. and Khair-Eldeen, W. (2011), "Powder metallurgical fabrication and microstructural investigations of aluminum/steel functionally graded material", *Mater. Sci. Appl.*, **2**(5), 1708-1718.
- Pei, G. and Asaro, R.J. (1997), "Cracks in functionally graded materials", *Int. J. Sol. Struct.*, **34**(1), 1-17.
- Petrov, V.V. (2014), *Non-Linear Incremental Structural Mechanics*, M.: Infra-Injeneria.
- Suresh, S. and Mortensen, A. (1998), *Fundamentals of Functionally Graded Materials*, IOM Communications Ltd., London, U.K.
- Szekrenyes, A. (2012), "J-integral for delaminated beam and plate models", *Period. Polytech. Mech. Eng.*, **56**(1), 63-71.
- Tilbrook, M.T., Moon, R.J. and Hoffman, M. (2005), "Crack propagation in graded composites", *Compos. Sci. Technol.*, **65**(2), 201-220.
- Upadhyay, A.K. and Simha, K.R.Y. (2007), "Equivalent homogeneous variable depth beams for cracked FGM beams; compliance approach", *Int. J. Fract.*, **144**(2), 209-213.
- Zhang, H., Li, X.F., Tang, G.J. and Shen, Z.B. (2013), "Stress intensity factors of double cantilever nanobeams via gradient elasticity theory", *Eng. Fract. Mech.*, **105**(1), 58-64.